

Appendix A

Figure A1.

Study Timeline.

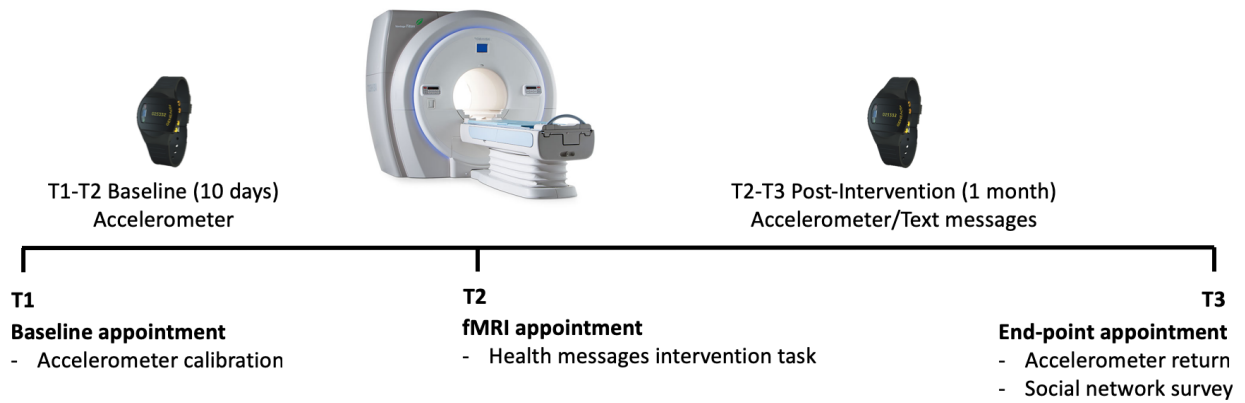
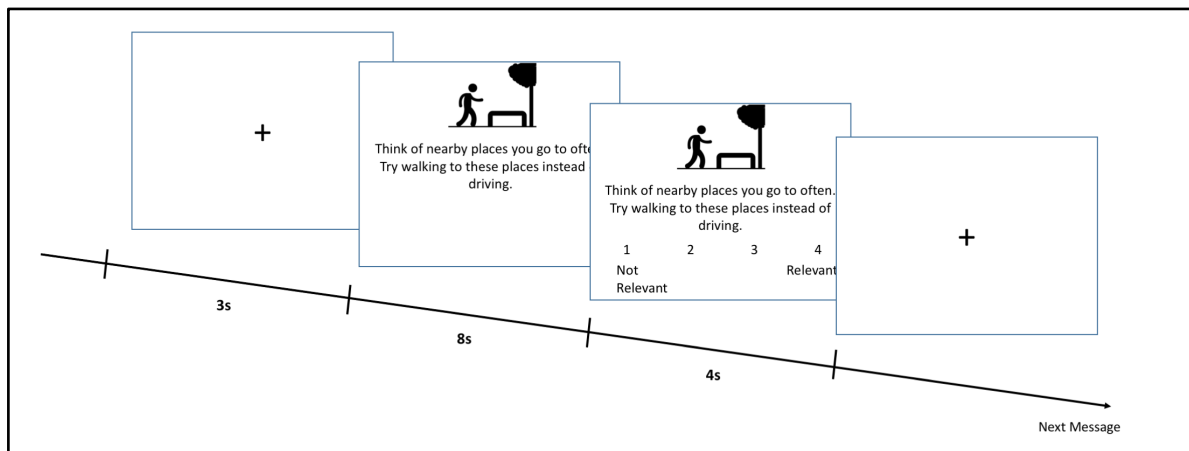


Figure A2.

Example Block from the Health Messages Intervention Task



Appendix B

The following section of fMRI data acquisition and data processing is a direct excerpt from Kang et al. (2018), the parent dataset for the current research, reproduced here for ease of review and reader comprehension.

fMRI Data Acquisition and Data Processing.

The imaging data were acquired on a 3 Tesla Siemens Trio scanner equipped with a 32 or 64 channel head coil (head coil type was not associated with VMPFC activity; $p = 0.65$). Participants were self-guided through two runs of the messages task (run1=376, run2=344 volumes, 720 volumes total), embedded among four other tasks not reported here (Refer to <https://github.com/cnlab/PhysicalActivity2> for details on other tasks). High-resolution T1-weighted structural images were collected using an MPRAGE sequence (TI=1,100ms, 160 slices, slice thickness=1mm, voxel size=0.9 x 0.9 x 1). To capture brain activity during tasks, T2*-weighted functional images were recorded (repetition time=1,500ms, echo time=25ms, flip angle=70°, -30° tilt relative to AC-PC line, 54 slices, field of view=200mm, slice thickness=3mm, multiband acceleration factor=2, voxel size=3.0 x 3.0 x 3.0 mm).

The anatomical and functional data were acquired and preprocessed using a standard processing stream using Statistical Parametric Mapping (SPM8; Wellcome Department of Cognitive Neurology, Institute of Neurology, London, UK) for all stages apart from the initial despiking, which was carried out using the 3dDespike program as implemented in the AFNI toolbox. Differences in time of acquisition were corrected using a sinc interpolation algorithm with the first slice as reference. Next, data were spatially realigned to the first slice of each volume, and co-registered to functional and

structural images using two six-parameter affine stages. The mean image across all blood oxygen level-dependent (BOLD) functional images was registered to high-resolution T1 images (total of 12 parameter affine).

Following coregistration, the high-resolution T1 images were segmented into gray matter, white matter and cerebrospinal fluid to create a brain mask used to determine voxels to be included in first and second-level models. Structural and functional images were then normalized to the skull-stripped MNI template ("MNI152_T1_1mm_brain.nii") provided by the FMRIB Software Library (FSL). In the final preprocessing step, the functional images were smoothed using a Gaussian kernel (8-mm FWHM). To allow for the stabilization of the BOLD signal, the first five volumes (7.5s) of each run were discarded before analysis. Movement parameters (a total of six rigid-body parameters, three for translation and three for rotation) derived from spatial realignment were included as nuisance regressors in all first-level models. Data were high pass filtered with a cutoff of 128s.

The following section of accelerometer calibration and preprocessing is an adapted excerpt from Kang et al. (2018), the parent dataset for the current research, reproduced here with some edits in brackets for ease of review and reader comprehension.

Accelerometer calibration and preprocessing

Participants were directed to wear the waterproof GENE A accelerometer at all times. As part of the baseline accelerometer calibration, participants performed sedentary (i.e., completing surveys while seated at a computer terminal for at least 30 min) and moderate/vigorous activities (walking/climbing up and down the stairs for 6 min). For

SOCIAL NETWORK INFLUENCE ON HEALTH MESSAGE RECEPTIVITY

each participant, the third quartile (75th percentile) of the activity during the sedentary period was used as a sedentary threshold, such that activity below that threshold was tagged as “sedentary.” Activity greater than the second quartile (50th percentile) of the peak level during the moderate/vigorous period was tagged as “moderate/vigorous.” (These cut-points were inspired by the idea that personalized cut points can be beneficial for this type of research (Ozemek et al., 2013), and consistent with research calibration studies using GENEActiv (Esliger et al., 2011) and Actigraph (Ozemek et al., 2013) accelerometers.)

Using the epoch converter function in the GENEActiv software, the raw triaxial data recorded at 20Hz were downsampled to 1 minute epochs, and the Sum Vector Magnitude (an integration of x, y and z acceleration) was used to provide an activity intensity score (for each minute). Periods in which participants were sleeping or were not wearing the accelerometers were tagged by three research assistants blind to study hypotheses and condition assignments and excluded from the analysis. During the remaining periods in which participants were awake and wearing the device, days with less than 5 hours of wear were excluded (6,242 days of 7,092 tagged, or 88%, met this criterion).

Average daily proportions of activity during the T1-T2 baseline and T2-T3 post intervention periods were computed by dividing the durations (i.e., number of usable minutes) of moderate/vigorous and sedentary times, separately, by the total usable time that excludes sleep and non-wear time for each day (tagged by three blind coders). (These daily scores were averaged across the ten-day baseline (pre-average) and one-month post-intervention periods (post-average). Pre to post-intervention change

SOCIAL NETWORK INFLUENCE ON HEALTH MESSAGE RECEPTIVITY

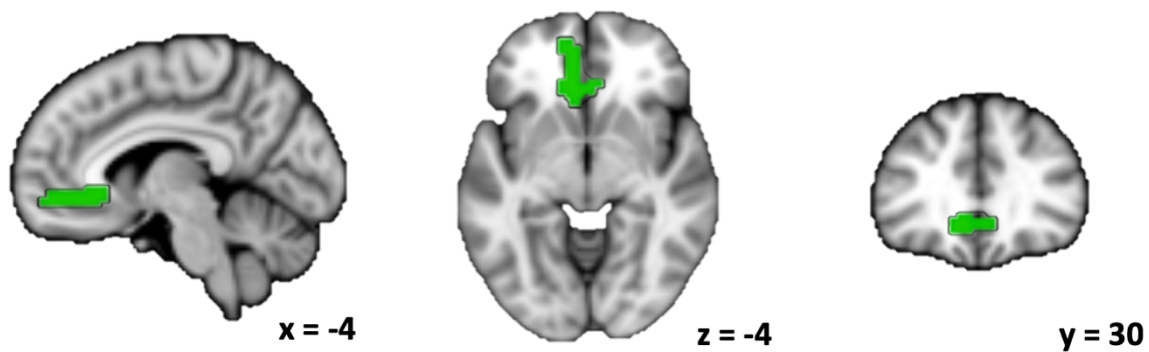
scores were computed by subtracting average pre (i.e., baseline) intervention proportion scores from post-intervention proportion scores.)

Whole Brain Analysis.

A whole brain analysis was conducted to identify brain regions associated with behavior change in the current useable dataset, using beta estimates from the first level models, which contrasted exposure to 30 health messages to rest during the health messages intervention task. Using the nistats toolbox in the Python programming language (<https://nistats.github.io/>), a second level design matrix was designed where each participant was weighted by their percentage change in sedentary minutes. After fitting brain data to the second level model, the map was thresholded with false positive rate (FPR) correction at $\alpha < 0.005$ ($t > 2.58$) to identify clusters significantly associated with decreases in sedentary behavior. A cluster in VMPFC (k=67) was identified that extends near ventral striatum (VS) which was associated with decreases in sedentary behavior (Figure A1).

Figure A3.

VMPFC and VS ROI Associated with Decreases in Sedentary Behavior



Sagittal, axial and coronal views of VMPFC and VS region-of-interest, with activations correlated with decrease in sedentary behavior, identified in whole brain analysis, FPR corrected cluster at $\alpha < 0.005$.

Appendix C

Aggregate Norms Correlated with Social Network Norms.

Aggregate norms about physical activity were measured using questions adapted from Fishbein et al. (1992): “What percentage of your friends are in the process of increasing daily physical activity?” (0-100%); “What percentage of people in general are in the process of increasing their daily physical activity?” (0-100%). The relationships between social network norms and each measure of aggregate norms were tested. Across the measures reported for the three visits, social network norms consistently showed a positive and statistically significant correlation with aggregate norms about friends’ physical activity, $p < 0.01$ (see Table A1). However, no significant association was found between aggregate norms¹ and neural receptivity in VMPFC, $p > 0.58$ (see Table A2).

Social Network Characteristics Associated with Regions Predictive of Behavior Change.

Further analysis tested links between social network characteristics and brain activity within regions associated with decreases in sedentary behavior, as identified by the whole brain analysis (see Appendix B). Higher social network norms about physical activity were marginally associated with greater increases in activations within these regions, $R^2 = .05$, $\beta = 0.14$, $t(142) = 1.68$, $p = .10$, 95% CI [-0.01, 0.06]. Higher closeness to physically inactive social ties was associated with greater decreases in activations within these regions, $R^2 = 0.06$, $\beta = -.17$, $t(137) =$

¹ Even though social network norms and aggregate norms are significantly correlated, there are substantive differences between the two measures. Our measure of aggregate norms assessed perceptions of health behavior at an aggregate group level. By contrast, our measure of social network norms guided respondents to think about the behavior of individual friends in their networks, which we then aggregated into a measure of the cumulative effect of individual behaviors on perceived social network norms. Additionally, our measure of aggregate norms focused on dynamic change processes (i.e., what proportion of friends are in the process of changing; Sparkman & Walton, 2017). By contrast, our social network norm measure focused on assessing perceptions of current peer behavior. Future research that disentangles the effects of these different components on neural receptivity to health messaging will be of value.

SOCIAL NETWORK INFLUENCE ON HEALTH MESSAGE RECEPTIVITY

-2.05, $p = .04$, 95% CI [-0.04, 0.00]. Closeness to physically active social ties was not associated with change in activations within these regions, $R^2 = 0.03$, $\beta = -.01$, $t(138) = -0.15$, $p = .88$, 95% CI [-0.02, 0.02]. These results are consistent with the results reported in the main manuscript using an overlapping region of VMPFC.

Social Network Norms and Physical Activity

Participants did not show an overall significant decrease in daily proportion of sedentary minutes ($t=0.174$, $p=0.862$). Baseline minutes of sedentary behavior were not associated with social network norms of physical activity, $R^2 = .01$, $\beta = 0.04$, $t(149) = 0.43$, $p = .67$, 95% CI [-0.03, 0.04], closeness to physically active social ties, $R^2 = .01$, $\beta = 0.02$, $t(145) = 0.23$, $p = .82$, 95% CI [-0.02, 0.02], or closeness to physically inactive social ties, $R^2 = 0.01$, $\beta = -0.02$, $t(141) = -0.27$, $p = .79$, 95% CI [-0.02, 0.02].

SOCIAL NETWORK INFLUENCE ON HEALTH MESSAGE RECEPTIVITY

Table A1.

Correlations between Social Network Norms and Aggregate Norms.

	Social Network Norms					
	T1 visit		T2 visit		T3 visit	
	r	p-value	r	p-value	r	p-value
“What percentage of your friends are in the process of increasing their daily physical activity?”	0.191	0.013	0.236	0.002	0.219	0.005
“What percentage of people in general are in the process of increasing their daily physical activity?”	0.080	0.302	0.179	0.021	0.062	0.427

Note. Pearson product-moment correlations between social network norms and aggregate norms physical activity for all three laboratory visits.

Table A2.

Correlations between VMPFC activity and Aggregate Norms.

	Percentage activity change in VMPFC (Falk et al., 2010)					
	T1 visit		T2 visit		T3 visit	
	r	p-value	r	p-value	r	p-value
“What percentage of your friends are in the process of increasing their daily physical activity?”	0.012	0.866	0.041	0.581	0.017	0.822
“What percentage of people in general are in the process of increasing their daily physical activity?”	-0.016	0.831	-0.022	0.763	0.003	0.970

Note. Pearson product-moment correlations between percentage change in activity in VMPFC ROI defined by Falk et al. (2010) and aggregate norms about physical activity, at all three laboratory visits.

SOCIAL NETWORK INFLUENCE ON HEALTH MESSAGE RECEPTIVITY

Table A3.

Association between Social Network Norms and Neural Activity

	Percentage change in neural activity							
	(1) VMPFC (Falk et al., 2010)				(2) VMPFC and VS (whole brain analysis)			
	Std. β	p-value (t-value)	Std. β	p-value (t-value)	Std. β	p-value (t-value)	Std. β	p-value (t-value)
Social Network Norms	0.169	.043 (2.043)	0.171	.042 (2.051)	0.139	.096 (1.677)	0.143	.090 (1.707)
<i>Demographics and control</i>								
Facebook API	-0.167	.048 (-1.998)	-0.132	.148 (-1.456)	-0.137	.106 (-1.627)	-0.104	.255 (-1.144)
Priming condition	-0.037	.656 (-0.446)	-0.043	.613 (-0.507)	-0.090	.284 (-1.075)	-0.096	.262 (-1.126)
Age	-	-	-0.062	.465 (-0.733)	-	-	-0.049	.562 (-0.582)
Gender	-	-	-0.033	.693 (-0.396)	-	-	-0.026	.756 (-0.312)
Race (ref=Black)	-	-	0.049	.594 (0.534)	-	-	0.076	.409 (0.828)
Years of education	-	-	0.093	.308 (1.024)	-	-	0.052	.573 (0.565)
R^2	.054		.071		.047		.061	

Note. Association between social network norms with neural activity in (1) VMPFC ROI defined by Falk et al. (2010), (2) functionally defined regions in VMPFC associated with decrease in sedentary behavior, controlled for priming conditions, demographic variables, and if the participant used the Facebook Graph API.

SOCIAL NETWORK INFLUENCE ON HEALTH MESSAGE RECEPTIVITY

Table A4.

Association between Closeness to Physically Inactive Social Ties and Neural Activity

	Percentage change in neural activity							
	(1) VMPFC (Falk et. al., 2010)				(2) VMPFC and VS (whole brain analysis)			
	Std. β	p-value (t-value)	Std. β	p-value (t-value)	Std. β	p-value (t-value)	Std. β	p-value (t-value)
Closeness to physically inactive social ties	-0.206	.015 (-2.452)	-0.201	.019 (-2.373)	-0.172	.043 (-2.045)	-0.165	.054 (-1.942)
<i>Demographics and control</i>								
Facebook API	-0.158	.069 (-1.832)	-0.124	.179 (-1.351)	-0.165	.058 (-1.914)	-0.132	.155 (-1.430)
Priming condition	-0.047	.577 (-0.559)	-0.044	.614 (-0.505)	-0.080	.351 (-0.936)	-0.080	.359 (-0.920)
Age	-	-	-0.011	.898 (-0.128)	-	-	-0.023	.793 (-0.263)
Gender	-	-	-0.058	.498 (-0.679)	-	-	-0.040	.642 (-0.466)
Black	-	-	0.047	.605 (0.519)	-	-	0.075	.412 (0.822)
Years of education	-	-	0.089	.334 (0.970)	-	-	0.061	.511 (0.659)
R^2	.061		.078		.058		.073	

Note. Association between closeness to physically inactive social ties with neural activity in (1) VMPFC ROI defined by Falk et al. (2010), (2) functionally defined regions in VMPFC associated with decrease in sedentary behavior, controlled for priming conditions, demographic variables, and if the participant used the Facebook Graph API.